Intermediate filaments exchange subunits along their length and elongate by end-to-end annealing

Gülsen Çolakoğlu[1,2] and Anthony Brown[1,2]

[1]Center for Molecular Neurobiology and [2]Department of Neuroscience, The Ohio State University, Columbus, OH 43210

Actin filaments and microtubules lengthen and shorten by addition and loss of subunits at their ends, but it is not known whether this is also true for intermediate filaments. In fact, several studies suggest that in vivo, intermediate filaments may lengthen by end-to-end annealing and that addition and loss of subunits is not confined to the filament ends. To test these hypotheses, we investigated the assembly dynamics of neurofilament and vimentin intermediate filament proteins in cultured cells using cell fusion, photobleaching, and photoactivation strategies in combination with conventional and photoactivatable fluorescent fusion proteins. We show that neurofilaments and vimentin filaments lengthen by end-to-end annealing of assembled filaments. We also show that neurofilaments and vimentin filaments incorporate subunits along their length by intercalation into the filament wall with no preferential addition of subunits to the filament ends, a process which we term intercalary subunit exchange.

Introduction

Actin filaments and microtubules exist in dynamic equilibrium with a soluble subunit pool, and it is well established that these polymers lengthen and shorten by addition and loss of subunits at their ends. Intermediate filaments also exchange subunits with a soluble subunit pool (Albers and Fuchs, 1987; Angelides et al., 1989), but, remarkably, the site of subunit exchange is not clear (Alberts et al., 2002; Kim and Coulombe, 2007; Godsel et al., 2008; Lodish et al., 2008). In fact, several studies have suggested that subunit exchange is not confined to the ends of intermediate filaments and that these polymers can exchange subunits along their length (Ngai et al., 1990; Coleman and Lazarides, 1992; Vikstrom et al., 1992). In addition, observations on vimentin and keratin filaments in living cells suggest that they may elongate by end-to-end annealing in vivo (Prahlad et al., 1998; Woll et al., 2005), and this is supported by studies using electron microscopy and mathematical modeling in vitro (Herrmann et al., 1999; Wickert et al., 2005; Kirmse et al., 2007).

In this study, we describe experiments that directly test the mechanisms of lengthening and subunit exchange of cytoplasmic intermediate filaments in cultured cells. We have focused on vimentin and neurofilament proteins, which are members of the type III and IV families of intermediate filament proteins, respectively (Coulombe and Wong, 2004). Vimentin forms homopolymers, whereas neurofilaments are obligate heteropolymers that are minimally comprised of the low molecular neurofilament protein L (NFL) plus the medium and/or high molecular weight proteins neurofilament protein M (NFM) and neurofilament protein H (NFH; Lee et al., 1993).

Results and discussion

To test the hypothesis that intermediate filaments can anneal end-to-end, we have taken advantage of the SW13 vim$^-$ human adrenal carcinoma cell line, which lacks endogenous cytoplasmic intermediate filaments because of spontaneous silencing of vimentin expression (Sarria et al., 1990; Yamamichi-Nishina et al., 2003). We cotransfected SW13 vim$^-$ cells with either NFL plus EGFP-tagged NFM to form green fluorescent neurofilaments or with NFL plus mCherry-tagged NFM to form red fluorescent neurofilaments. We then mixed the cells and fused them with polyethylene glycol (PEG) to create cells containing distinct populations of red and green filaments (Fig. 1, a and b). Alternatively, to confirm our data with a strategy that does not involve cell fusion, we cotransfected cells with NFL plus photoactivatable GFP (PAGFP)–tagged NFM and mCherry-tagged NFM to form a single population of neurofilaments containing

Correspondence to Anthony Brown: brown.2302@osu.edu

Abbreviations used in this paper: NFH, neurofilament protein H; NFL, neurofilament protein L; NFM, neurofilament protein M; PAGFP, photoactivatable GFP; PEG, polyethylene glycol; ULF, unit length filament.

The Rockefeller University Press $30.00
J. Cell Biol. Vol. 185 No. 5 769–777
www.jcb.org/cgi/doi/10.1083/jcb.200809166

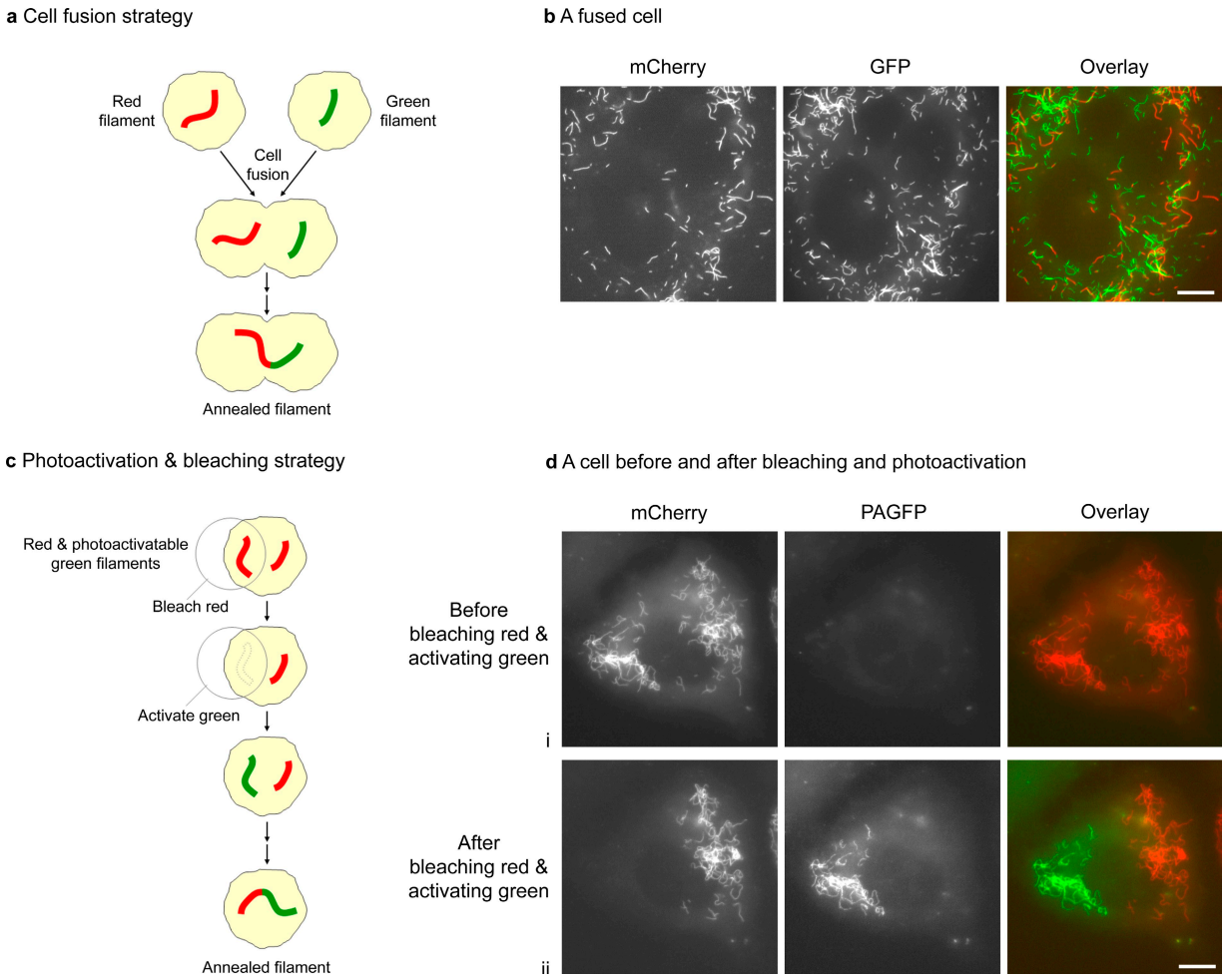

Figure 1. **Strategies to test for end-to-end annealing of intermediate filaments.** (a) Schematic of the cell fusion strategy. (b) A cell obtained by fusion of SW13 vim$^-$ cells coexpressing NFM-mCherry and NFL with SW13 vim$^-$ cells coexpressing NFM-GFP and NFL and imaged 3.5 h after fusion. (c) Schematic of the photoactivation and bleaching strategy. (d) An SW13 vim$^-$ cell coexpressing mCherry-NFM, PAGFP-NFM, and NFL imaged before bleaching and photoactivation (i), and immediately after bleaching and photoactivation before the filaments had mixed (ii). Bars, 10 µm.

both red and photoactivatable green fluorescence along their entire length. To create distinct populations of green and red filaments in these cells, we then bleached the red fluorescence in part of the cell and activated the green fluorescence in the same region (Fig. 1, c and d). With both of these strategies, we looked for the formation of chimeric filaments composed of contiguous green and red segments.

Both of these experimental strategies resulted in the appearance of filaments containing alternating contiguous red and green segments within several hours, which is indicative of end-to-end annealing. We obtained the same result with N- or C-terminally tagged NFM (each coexpressed with untagged NFL; Fig. 2, a, b, and d) and with N- or C-terminally tagged NFL (each coexpressed with untagged NFM; not depicted) as well as with N-terminally tagged vimentin (coexpressed with untagged vimentin; Fig. 2 c) and untagged neurofilament proteins (Fig. 2 f). To establish that the contiguous red and green segments were indeed part of the same filament, we took advantage of the fact that the filaments undergo constant Brownian-like motion, presumably caused by the thermal motion of their environment as well as jostling by other actively moving organelles in the cytoplasm. For each chimeric filament, we routinely acquired several consecutive images over a period of 10–15 min. In each case, the red and green segments remained contiguous at all times, confirming that they were part of the same filament (Fig. 2 e and Videos 1 and 2). In rare instances, we even observed circular filaments, which is indicative of annealing between two ends of the same filament (Video 3).

We also observed end-to-end annealing for N-terminally tagged NFM (coexpressed with untagged NFL) and N-terminally tagged vimentin (coexpressed with untagged vimentin) in MFT-16 cells, which are an immortalized fibroblast cell line derived from vimentin knockout mice (Fig. S1; Holwell et al., 1997), and in SW13 vim$^+$ cells stably transfected with N-terminally tagged vimentin (Fig. 2, g and h). Thus, end-to-end annealing is not an artifact of fusion proteins or transient transfection, is not unique to SW13 cells, and also occurs in the context of an endogenous intermediate filament network.

To quantify the annealing frequency, we measured the length and number of chimeric and nonchimeric filaments in SW13 vim$^-$ cells processed using the cell fusion strategy. For neurofilaments, 14% showed at least one annealing event (defined as a red/green junction) 2–5 h after fusion (n = 991 filaments from

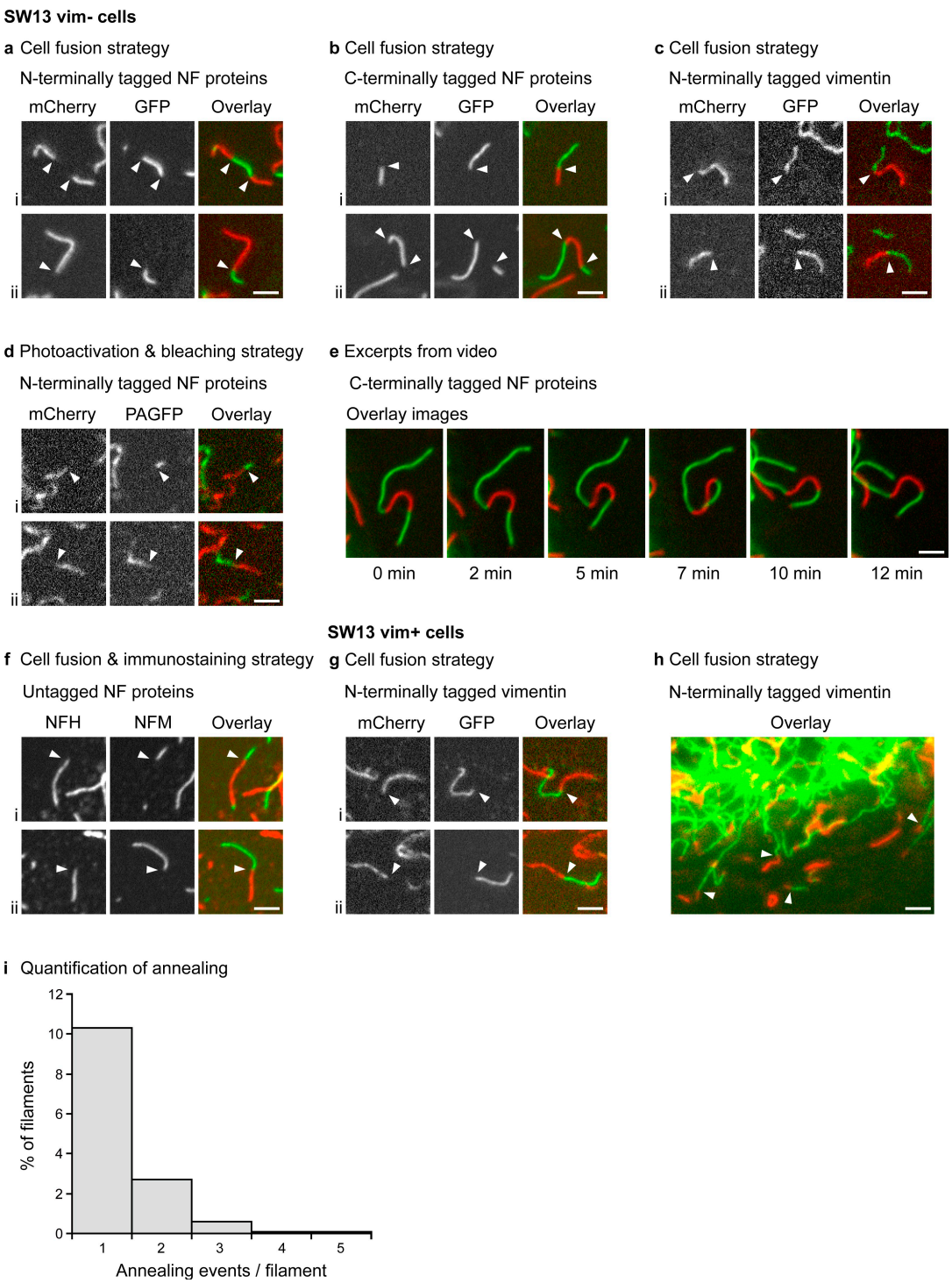

Figure 2. **Intermediate filaments undergo end-to-end annealing.** Sites of end-to-end annealing (red/green junctions) are marked with white arrowheads. Two examples (i and ii) are shown for each experiment. For clarity, we selected isolated filaments for most of the images. (a) Obtained by fusion of SW13 vim$^-$ cells coexpressing mCherry-NFM and NFL with SW13 vim$^-$ cells coexpressing GFP-NFM and NFL. (b) Obtained by fusion of SW13 vim$^-$ cells coexpressing NFM-mCherry and NFL with SW13 vim$^-$ cells coexpressing NFM-GFP and NFL. (c) Obtained by fusion of SW13 vim$^-$ cells coexpressing mCherry-vimentin and untagged vimentin with SW13 vim$^-$ cells coexpressing GFP-vimentin and untagged vimentin. (d) Obtained by photoactivation and bleaching of SW13 vim$^-$ cells coexpressing mCherry-NFM, PAGFP-NFM, and NFL. (e) Excerpts from a video of a neurofilament in a cell formed by the fusion of an SW13 vim$^-$ cell coexpressing NFM-GFP and NFL with an SW13 vim$^-$ cell coexpressing NFM-mCherry and NFL (Video 1). (f) Obtained by fusion of SW13 vim$^-$ cells coexpressing NFM and NFL with SW13 vim$^-$ cells coexpressing NFH and NFL. 5 h after fusion, the cells were fixed and immunostained for NFH and NFM. (g) Obtained by fusion of SW13 vim$^+$ cells stably expressing mCherry-vimentin with SW13 vim$^+$ cells stably expressing GFP-vimentin. (h) The edge of a cell obtained by fusion of SW13 vim$^+$ cells stably expressing mCherry-vimentin with SW13 vim$^+$ cells stably expressing GFP-vimentin. (i) Frequency distribution of the number of annealing events per filament 2–5 h after fusion of SW13 vim$^-$ cells coexpressing NFM-GFP and NFL with SW13 vim$^-$ cells coexpressing NFM-mCherry and NFL (991 filaments counted in five cells). NF, neurofilament. Bars, 2 μm.

five cells; Fig. 2 i), and the mean number of red/green junctions per chimeric filament was 1.3. The mean length of these chimeric filaments was 2.1 times longer than the nonchimeric filaments (4.9 µm and 2.3 µm, respectively; $n = 776$ filaments), confirming that annealing results in filament elongation. However, these numbers probably underestimate the full extent of annealing and lengthening because we can only detect annealing between filaments that are different colors. For vimentin filaments, 13% showed at least one annealing event 2–5 h after fusion ($n = 561$ filaments from five cells; unpublished data), and the mean number of red/green junctions per chimeric filament was 1.2. Collectively, these data indicate that neurofilaments and vimentin filaments are both capable of end-to-end annealing in these cells and that this process is remarkably efficient.

To test the hypothesis that preassembled intermediate filaments exchange subunits along their length, we cotransfected SW13 vim$^-$ cells with either NFL plus PAGFP-tagged NFM to form photoactivatable green fluorescent neurofilaments or with NFL plus mCherry-tagged NFM to form red fluorescent neurofilaments. We then mixed the cells and fused them to create cells containing distinct populations of red and photoactivatable green filaments. 1–5 h later, we activated the green fluorescence to mark the PAGFP-tagged filaments (Fig. 3, a and b). Alternatively, to confirm the data with a strategy that does not involve cell fusion, we also cotransfected cells with NFL plus PAGFP-tagged NFM and mCherry-tagged NFM to form neurofilaments containing both red and photoactivatable green fluorescence along their entire length. We then bleached the red fluorescence in the entire cell and activated the green fluorescence in a part of that cell to mark a subpopulation (5–30%) of the PAGFP-tagged filaments (Fig. 3, c and d), thereby creating a population of green fluorescent filaments lacking red fluorescence. In both cases, we looked for the incorporation of newly synthesized red fluorescent subunits along the photoactivated green fluorescent filaments.

Both of these experimental strategies resulted in the appearance of chimeric filaments within several hours after photoactivation, as described above. However, by 8 h after photoactivation, we also began to observe the appearance of red fluorescence along the photoactivated green filaments, which indicates that red fluorescent subunits had incorporated into the green filaments. We obtained the same result using N-terminally tagged NFM (coexpressed with untagged NFL) or C-terminally tagged NFL (coexpressed with untagged NFM; Fig. 4, a, b, and d) and also using N-terminally tagged NFL (coexpressed with untagged NFM; not depicted) or N-terminally tagged vimentin (coexpressed with untagged vimentin; Fig. 4 c). We also obtained the same result in MFT-16 cells expressing N-terminally tagged vimentin (coexpressed with untagged vimentin) or N-terminally tagged NFM (coexpressed with untagged NFL; Fig. S2) and in SW13 vim$^+$ cells stably expressing N-terminally tagged vimentin (Fig. 4 e). Thus, the capacity of preformed intermediate filaments to incorporate subunits along their length is not unique to SW13 cells and can also occur in the context of an endogenous intermediate filament network.

Some filaments exhibited patchy incorporation, but for most, the incorporation was relatively uniform. In many cases, this occurred along the photoactivated green portions of chimeric filaments (Fig. 4 b, example ii), which indicates that subunit incorporation and end-to-end annealing often occur along the same filament. In some cases, we observed segments of red fluorescence on one or both ends of a photoactivated green filament, which could be the result of de novo assembly on the filament ends or the result of annealing. However, the fact that we also observed photoactivated green fluorescent segments on one or both ends of a red filament argues that it reflects end-to-end annealing. Moreover, many photoactivated green filaments showed incorporation of red fluorescence along their length with no red fluorescence at their ends. Thus, neurofilaments and vimentin filaments are both capable of incorporating subunits along their length, and, in contrast to actin filaments and microtubules, there is no indication of preferential addition of subunits to the polymer ends.

To determine the extent of subunit incorporation along the filaments, we quantified the red and green fluorescence intensities of single neurofilaments in SW13 vim$^-$ cells using the cell fusion strategy (Fig. 4, g and h). Immediately after photoactivation (t = 0), the cells contained a mixture of red and photoactivated green fluorescent filaments, with no green fluorescence on the red filaments and no red fluorescence on the green filaments. By 20 h after photoactivation, the mean intensity of the red fluorescence on the green fluorescent filaments had increased to 20% of the mean intensity of the red fluorescent filaments at the start of the experiment (however, note that this increase is expected to underestimate the full extent of subunit incorporation because any incorporation of newly synthesized photoactivatable subunits, which are not fluorescent, would go undetected). This increase in red fluorescence was accompanied by a decrease in green fluorescence, which is consistent with an exchange of subunits between the filaments and the subunit pool. However, we observed no significant increase in green fluorescence along the red fluorescent filaments, which indicates that there was no significant pool of photoactivated green fluorescent subunits in these cells. This confirms that the green fluorescent filaments were the same ones that existed at the time of photoactivation and that the incorporation of red fluorescent subunits along the length of the green fluorescent neurofilaments cannot be explained by de novo assembly. We also quantified the time course of end-to-end annealing in these same cells. The proportion of filaments that were chimeric was 16% after 2–4 h ($n = 850$ filaments), 48% after 10–12 h ($n = 639$ filaments), and 58% after 16–24 h ($n = 712$ filaments). The mean number of annealing events per chimeric filament was 1.2 after 2–4 h (max = 5), 1.8 after 10–12 h (max = 10), and 2.4 after 16–24 h (max = 14; Fig. 4 f). Thus, subunit incorporation and end-to-end annealing are concurrent time-dependent processes in these cells.

The aforementioned data provide the first direct demonstration that intermediate filaments can anneal end-to-end in cells. The structural basis for this process is of obvious interest. Intermediate filaments are assembled from tetramer subunits (Soellner et al., 1985), but the polymer structure is not well understood. The tetramers are believed to align in register, whereas the dimers that comprise these tetrameric units are staggered, giving rise to ~10-nm overhangs (for reviews see Herrmann and Aebi, 2004; Herrmann et al., 2007). It is possible that interdigitation

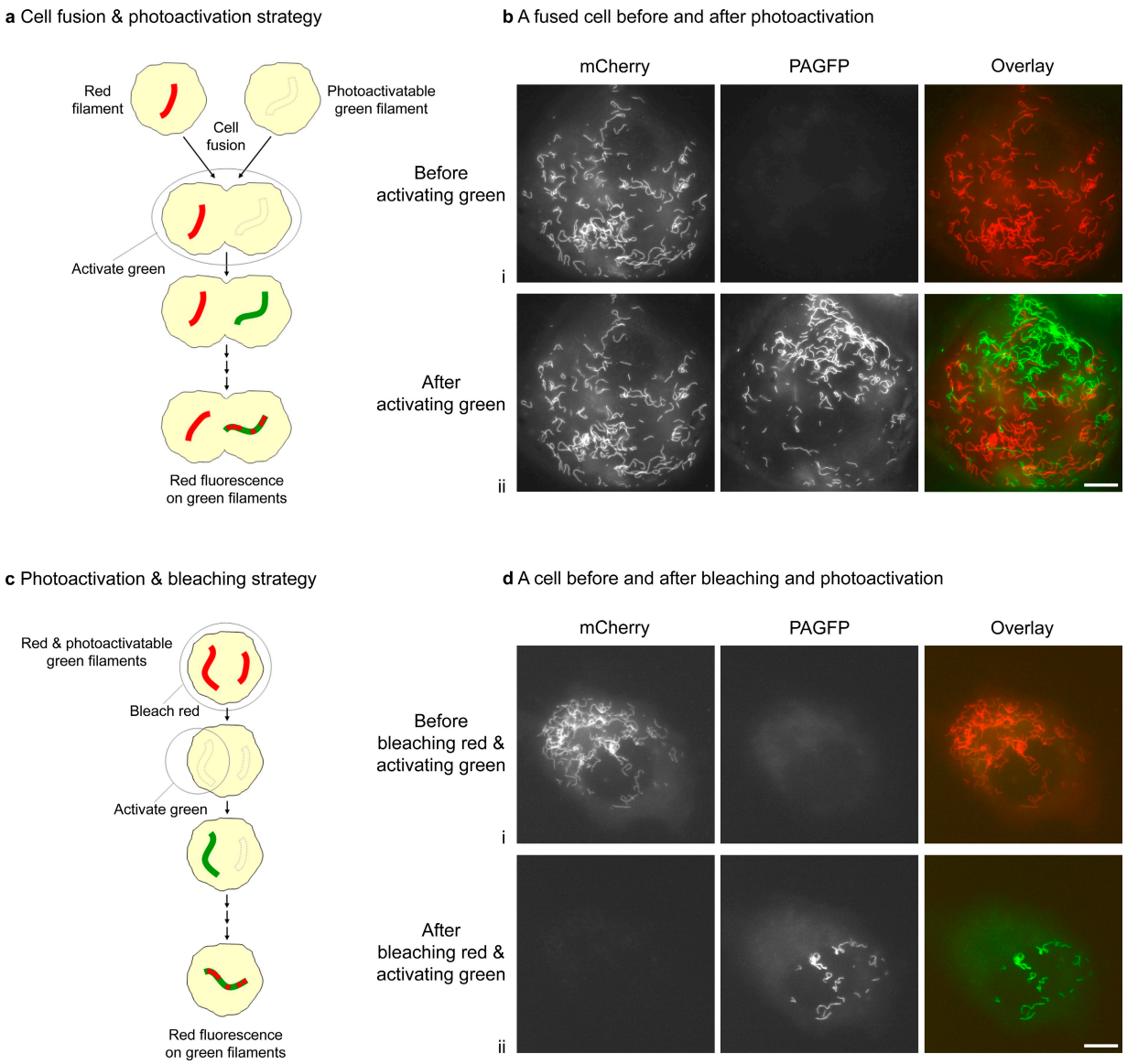

Figure 3. **Strategies to test for subunit incorporation along intermediate filaments.** (a) Schematic of the cell fusion and photoactivation strategy. (b) A cell obtained by fusion of SW13 vim$^-$ cells coexpressing NFL-PAGFP and NFM with SW13 vim$^-$ cells coexpressing NFL-mCherry and NFM and imaged before photoactivation (4.5 h after fusion; i) and immediately after photoactivation (ii). (c) Schematic of the photoactivation and bleaching strategy. (d) An SW13 vim$^-$ cell coexpressing mCherry-NFM, PAGFP-NFM, and NFL imaged before bleaching and photoactivation (i) and immediately after bleaching and photoactivation (ii). Bars, 10 μm.

of these protruding dimer overhangs at the filament ends may be critical for stabilizing the annealing junction (Fig. 5 a). The filaments have no structural polarity because the dimers within the tetramer subunits have an antiparallel orientation. Thus, the two ends of each filament are expected to be structurally identical and either end of one filament should be capable of annealing with either end of another.

In vitro, neurofilament and vimentin filament assembly proceeds via lateral aggregation of tetramer subunits to form short cylindrical assembly intermediates called unit length filaments (ULFs), which measure ~60 nm long and ~16 nm in diameter. ULFs have the same linear mass density as mature filaments but are thicker because they are less compact. Filament formation proceeds by end-to-end annealing of the ULFs to form thick filaments ~250 nm in length followed by further elongation and radial compaction to achieve a mature diameter of ~11 nm (Herrmann et al., 1996, 1999; Mucke et al., 2004; Wickert et al., 2005; Sokolova et al., 2006). Our data indicate that, in cells, end-to-end annealing can also occur between filaments that are several micrometers long, which have presumably become radially compacted. Thus, the capacity for end-to-end annealing may not be unique to assembly intermediates but may also apply to mature filaments. Moreover, the high frequency of annealing that we encountered in our experiments suggests that it is potentially a very efficient mechanism for filament elongation. This could be particularly important for neurofilaments, which have been reported to reach mean lengths in excess of 100 μm in axons (Burton and Wentz, 1992). End-to-end annealing has also been reported for microtubules and actin filaments in vitro (Rothwell et al., 1986; Murphy et al., 1988;

SW13 vim- cells

a Cell fusion & photoactivation strategy

N-terminally tagged NF proteins

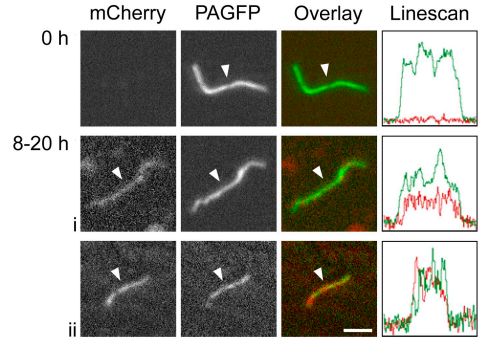

b Cell fusion & photoactivation strategy

C-terminally tagged NF proteins

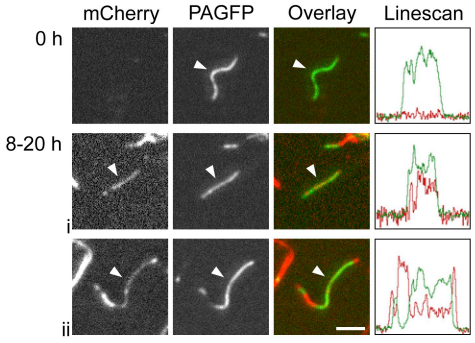

c Cell fusion & photoactivation strategy

N-terminally tagged vimentin

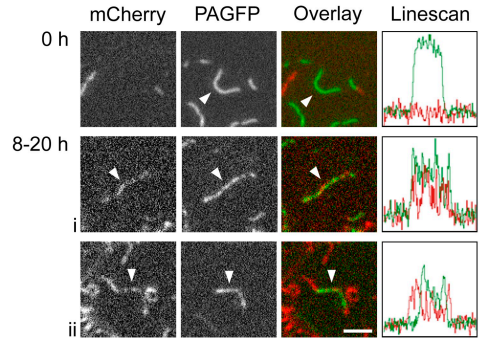

d Photoactivation & bleaching strategy

N-terminally tagged NF proteins

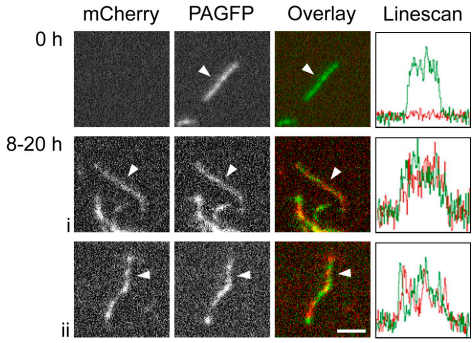

SW13 vim+ cells

e Cell fusion & photoactivation strategy

N-terminally tagged vimentin

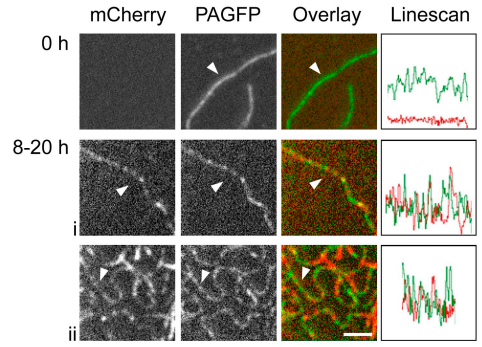

f Quantification of annealing

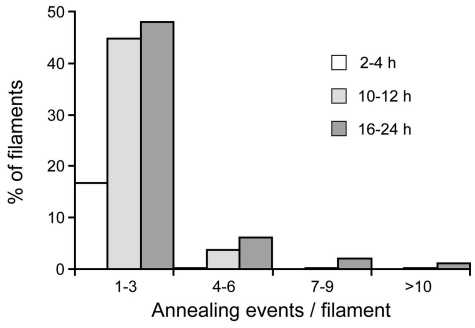

g Quantification of subunit exchange on green filaments

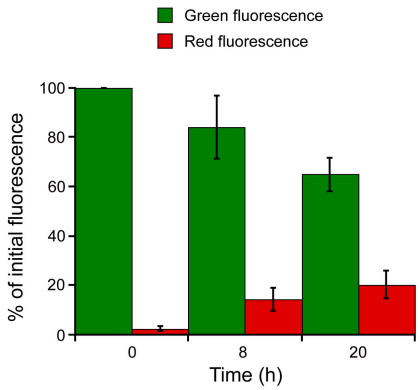

h Quantification of subunit exchange on red filaments

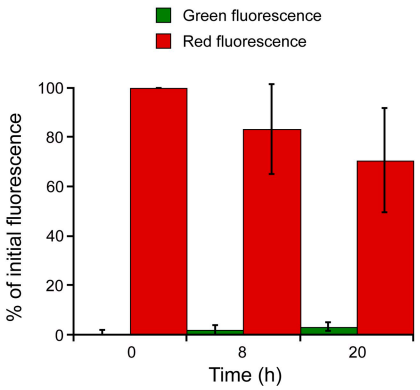

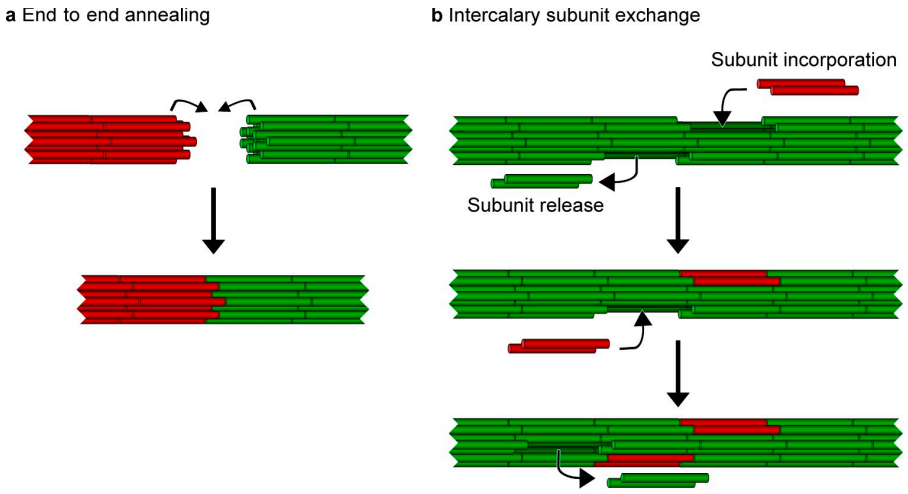

Figure 5. **Models for intermediate filament end-to-end annealing and intercalary subunit exchange.** The filaments are depicted as being composed of eight tetramers per cross section, each composed of two staggered coiled-coil dimers (shown as cylinders). (a) End-to-end annealing. For diagrammatic purposes, we show the end of a red filament annealing with the end of a green filament. The annealing mechanism may involve interdigitation of the protruding dimer overhangs at the filament ends. (b) Intercalary subunit exchange. For diagrammatic purposes, we show red tetramer subunits incorporating along the length of a green filament. Both annealing and intercalary subunit exchange may occur spontaneously in cells, although it is likely that there are also accessory factors that facilitate or regulate these processes.

Andrianantoandro et al., 2001), but, to the best of our knowledge, our data are the first direct demonstration of cytoskeletal polymer annealing in cells.

Comparative studies on intermediate filaments have identified three different assembly groups that differ in their stability and kinetics of assembly in vitro (for review see Herrmann and Aebi, 2004). These three intermediate filament systems can coexist in the same cell without coassembling. Our data demonstrate that neurofilaments and vimentin filaments (assembly group 2) can exchange subunits along their length, but it remains to be seen whether keratins and nuclear lamins (assembly groups 1 and 3) exhibit similar behavior. The time course of subunit exchange appears to be slow relative to the rates of subunit exchange in microtubules and microfilaments, but this is consistent with prior studies on subunit turnover in intermediate filament networks (Ngai et al., 1990; Coleman and Lazarides, 1992). Thus, intermediate filaments, although dynamic, are considerably less dynamic than their other cytoskeletal counterparts.

The structural implications of subunit exchange along the length of preexisting filaments were articulated eloquently by Ngai et al. (1990), Coleman and Lazarides (1992), and Vikstrom et al. (1992) >15 yr ago. These authors recognized that addition and loss of subunits along the wall of intermediate filaments would require transient disruption of the filament architecture. To understand how this could occur without severing the filament, it is important to understand the unique structure and plasticity of intermediate filament polymers. In contrast to actin filaments and microtubules, which have an essentially invariant structure, intermediate filaments exhibit considerable polymorphism in their diameter and linear mass density, indicating that the architecture of these assemblies can accommodate different numbers and arrangements of subunits within the polymer wall, even along the same filament (for review see Herrmann and Aebi, 2004). This suggests that intermediate filaments have a topologically open architecture in which tetramer subunits may dissociate and reinsert within the polymer wall without compromising the interactions between the other subunits (Fig. 5 b; Parry et al., 2007). We propose the term intercalary subunit exchange to describe this process. An important consequence of this unique dynamic behavior is that it may permit turnover or alteration of the subunit composition of intermediate filament polymers without compromising their structural integrity.

Materials and methods

Molecular cloning

The neurofilament protein constructs were all created by cloning mouse NFL and NFM cDNAs into pEGFP-C or pEGFP-N plasmids (Clontech Laboratories, Inc.). The vimentin constructs were obtained in a similar manner using human vimentin cDNA (provided by R. Goldman, Northwestern University, Chicago, IL). Untagged constructs were obtained by excising the GFP sequence. Photoactivatable and red fluorescent constructs were obtained by replacing the EGFP sequence with the sequences for PAGFP (provided by G. Patterson, National Institute of Child Health and Human Development, Bethesda, MD; Patterson and Lippincott-Schwartz, 2002) or mCherry (provided by R. Tsien, University of California, San Diego, La Jolla, CA; Shaner et al., 2004), respectively. The linker lengths were 25 aa for the N-terminally tagged NFM fusion constructs, 15 aa for the C-terminally tagged NFM-EGFP fusion construct, 7 aa for the C-terminally tagged NFM-mCherry fusion construct, 5 aa for the C-terminally tagged NFL fusion constructs, and 22 aa for the N-terminally tagged vimentin fusion constructs. All constructs were confirmed by DNA sequencing.

Figure 4. **Intermediate filaments incorporate subunits along their length.** The cells were imaged immediately after photoactivation (0 h) or 8–20 h later (examples i and ii). The line scans show the green and red fluorescence intensity profiles along the filaments indicated by the white arrowheads. For clarity, we selected isolated filaments for most of the images. (a) Obtained by fusion of SW13 vim$^-$ cells coexpressing PAGFP-NFM and NFL with SW13 vim$^-$ cells coexpressing mCherry-NFM and NFL. (b) Obtained by fusion of SW13 vim$^-$ cells coexpressing NFL-PAGFP and NFM with SW13 vim$^-$ cells coexpressing NFL-mCherry and NFM. (c) Obtained by fusion of SW13 vim$^-$ cells coexpressing PAGFP-vimentin and untagged vimentin with SW13 vim$^-$ cells coexpressing mCherry-vimentin and untagged vimentin. (d) Obtained by photoactivation and bleaching of SW13 vim$^-$ cells coexpressing PAGFP-NFM, mCherry-NFM, and NFL. (e) Obtained by fusion of SW13 vim$^+$ cells stably expressing PAGFP-vimentin with SW13 vim$^+$ cells stably expressing mCherry-vimentin. (f) Frequency distribution of the number of annealing events per filament at 2–4, 10–12, and 16–24 h after fusion for the same five cells analyzed in g and h (number of filaments counted = 850, 639, and 712, respectively). (g and h) Quantification of subunit exchange on green and red fluorescent filaments in cells obtained by the fusion of SW13 vim$^-$ cells coexpressing NFL-PAGFP and NFM with SW13 vim$^-$ cells coexpressing NFL-mCherry and NFM. Data are averaged from five different cells at 0, 8, and 20 h after PAGFP activation (at least 160 filaments per time point). The error bars represent mean ± standard deviation. NF, neurofilament. Bars, 2 μm.

Cell culture and transfection

SW13 and MFT-16 cells (provided by R. Evans, University of Colorado, Denver, Denver, CO; Sarria et al., 1990; Holwell et al., 1997) were plated on regular glass or etched glass coverslips (Bellco Biotechnology) in 35-mm culture dish assemblies and were maintained in DMEM/F12 (Invitrogen) supplemented with 5% FBS (HyClone) and 10 µg/ml gentamycin at 37°C and 5% CO_2. SW13 vim$^-$ cells were transiently transfected using Lipofectamine 2000 (Invitrogen) in serum-free DMEM/F12 medium. SW13 vim$^+$ cells were stably transfected with vimentin fusion constructs using Lipofectamine 2000 and then cultured in the presence of 1 mg/ml Geneticin (Invitrogen) for 4 wk, changing the medium every 2–3 d. The resulting stably transfected cells were maintained as a mixed clonal population and cultured in the presence of 200 µg/ml Geneticin. MFT-16 cells were transiently transfected by electroporation using a Nucleofector (Lonza). For experiments on neurofilaments, we cotransfected NFL in combination with NFM fusion proteins or NFM in combination with NFL fusion proteins, always maintaining a 1:1 ratio of NFL and NFM DNA. For experiments on vimentin, we cotransfected vimentin in combination with vimentin fusion proteins, always maintaining a 1:1 ratio of the tagged and untagged vimentin DNA.

Cell fusion

Separate dishes of cells expressing red or green fluorescent intermediate filaments were harvested 4–18 h after transfection and then mixed and replated at 30–50% confluency. After 8–18 h, the culture medium was aspirated completely from the dish and replaced with PEG solution prewarmed to 37°C. For the SW13 cells, we used 50% (wt/vol) PEG 1500 in 75 mM Hepes, pH 8.0 (Roche). 1 min later, the PEG solution was removed, and the cells were incubated for 1 min more. Prewarmed DMEM/F12 culture medium (containing FBS and gentamycin) was then added very slowly, and the cells were returned to the incubator. 1–2 h later, the medium was replaced with fresh medium. The procedure was the same for the MFT-16 cells except that we used 45% PEG and then, after 1 min, we added medium directly to the dish without removing the PEG. After three rinses with culture medium, the cells were kept for at least 1 h in the incubator before imaging.

Immunostaining

Cells were rinsed twice with PBS and fixed at 37°C for 15 min with 4% formaldehyde in PBS containing 1% sucrose. After fixation, the cells were rinsed again with PBS, permeabilized with 0.25% Triton X-100 in PBS at room temperature for 15 min, and then treated with blocking solution (4% normal goat serum in PBS; Jackson ImmunoResearch Laboratories). Immunostaining was performed using RMO-270 anti-NFM mouse monoclonal (1:100; Invitrogen) and AB1989 anti-NFH rabbit polyclonal (1:100; Millipore) primary antibodies followed by Alexa Fluor 488–conjugated goat anti–mouse (1:200; Invitrogen) and rhodamine red-X–conjugated goat anti–rabbit (1:200; Jackson ImmunoResearch Laboratories) secondary antibodies. Both primary and secondary antibodies were diluted in blocking solution, and the incubations were performed at 37°C for 45 min.

Microscopy and imaging

For imaging, the DMEM/F12 culture medium was replaced with Hibernate-E low fluorescence medium (Brain Bits). A layer of silicone fluid (5 centipoise polydimethylsiloxane; Sigma-Aldrich) was floated onto the medium to prevent evaporation during observation on the microscope stage. Imaging was performed using an inverted microscope (TE2000; Nikon) with a 100-W mercury lamp source and a 100× NA 1.4 Plan-Apochromat VC or 100× NA 1.4 Plan-Apochromat DM oil immersion objective. Images were acquired with a cooled charge-coupled device camera (CoolSNAP HQ; Roper Scientific) using MetaMorph software (MDS Analytical Technologies). The temperature on the microscope stage was maintained at ∼35°C using an air stream incubator (ASI-400; NevTek). mCherry was observed with an HQ-TRITC filter cube (model 41002b; Chroma Technology Corp.) or an ET–Texas red filter cube (model 49008; Chroma Technology Corp.). EGFP and activated PAGFP were observed with an HQ-FITC filter cube (model 41001; Chroma Technology Corp.) or an ET-GFP filter cube (model 49002; Chroma Technology Corp.). For the experiments with SW13 cells, the exciting light was attenuated eightfold or 12-fold with neutral density filters, and images were acquired with no pixel binning. For the experiments with MFT-16 cells, the exciting light was attenuated fourfold with neutral density filters, and images were acquired using a pixel binning factor of two. mCherry was photobleached by excitation for 1–2 min without neutral density filters. PAGFP was activated by illumination for 1 s without neutral density filters using a violet filter cube (model 11005v2; Chroma Technology Corp.). For partial cell activation, a field-limiting diaphragm in a conjugate focal plane of the epifluorescent illumination path was used to expose only a part of the cell to violet light. In later experiments, we used a Mosaic Digital Diaphragm (Photonic Instruments).

Analysis

To quantify the annealing frequency, we used the cell fusion strategy to create cells containing both red and green filaments and then counted the number of red/green junctions along every filament that could be resolved from its neighbors and for which at least one end was visible. To measure the lengths of chimeric and nonchimeric filaments, we confined our analyses to filaments for which both ends were visible. To quantify subunit incorporation along single filaments, we used the cell fusion strategy to create cells containing both red and photoactivatable green filaments. We then activated the PAGFP fluorescence 2–4 h after fusion and imaged the PAGFP and mCherry fluorescence immediately and after 8 and 20 h (t = 0, 8, and 20 h, respectively). We quantified the red and green fluorescence intensities of single filaments at all three time points and then normalized the red fluorescence intensities to the mean fluorescence intensity of the red fluorescent filaments at t = 0 and the green fluorescence intensities to the mean fluorescence intensity of the green fluorescent filaments at t = 0. In a parallel set of experiments, we determined that the extent of photobleaching over the time course of these experiments was <16% for the activated PAGFP fluorescence and <5% for the mCherry fluorescence. Intensity profiles along single filaments were obtained using the line scan function in MetaMorph software using a line width of 3 pixels.

Online supplemental material

Fig. S1 shows end-to-end annealing of neurofilaments and vimentin filaments in MFT-16 cells. Fig. S2 shows incorporation of subunits along the length of neurofilaments and vimentin filaments in MFT-16 cells. Videos 1 and 2 show examples of chimeric neurofilaments undergoing Brownian-like motion. Video 3 shows a rare example of a circular filament, which is indicative of self-annealing. Online supplemental material is available at http://www.jcb.org/cgi/content/full/jcb.200809166/DC1.

We thank Robert Evans for the SW13 and MFT-16 cells, Robert Goldman for the vimentin cDNA, George Patterson for the PAGFP cDNA, Roger Tsien for the mCherry cDNA, and Kitty Jensen in the Brown laboratory for cloning the mouse NFL and NFM cDNAs.

This project was funded by National Institutes of Health grant RO1-NS38526 to A. Brown. Additional support was provided by National Institutes of Health grant P30-NS045758.

Submitted: 23 September 2008
Accepted: 1 May 2009

References

Albers, K., and E. Fuchs. 1987. The expression of mutant epidermal keratin cDNAs transfected in simple epithelial and squamous cell carcinoma lines. *J. Cell Biol.* 105:791–806.

Alberts, B., A. Johnson, J. Lewis, M. Raff, K. Roberts, and P. Walter. 2002. Molecular Biology of the Cell. Fourth edition. Garland Science, New York. 1548 pp.

Andrianantoandro, E., L. Blanchoin, D. Sept, J.A. McCammon, and T.D. Pollard. 2001. Kinetic mechanism of end-to-end annealing of actin filaments. *J. Mol. Biol.* 312:721–730.

Angelides, K.J., K.E. Smith, and M. Takeda. 1989. Assembly and exchange of intermediate filament proteins of neurons: neurofilaments are dynamic structures. *J. Cell Biol.* 108:1495–1506.

Burton, P.R., and M.A. Wentz. 1992. Neurofilaments are prominent in bullfrog olfactory axons but are rarely seen in those of the tiger salamander, *Ambystoma tigrinum*. *J. Comp. Neurol.* 317:396–406.

Coleman, T.R., and E. Lazarides. 1992. Continuous growth of vimentin filaments in mouse fibroblasts. *J. Cell Sci.* 103:689–698.

Coulombe, P.A., and P. Wong. 2004. Cytoplasmic intermediate filaments revealed as dynamic and multipurpose scaffolds. *Nat. Cell Biol.* 6:699–706.

Godsel, L.M., R.P. Hobbs, and K.J. Green. 2008. Intermediate filament assembly: dynamics to disease. *Trends Cell Biol.* 18:28–37.

Herrmann, H., and U. Aebi. 2004. Intermediate filaments: molecular structure, assembly mechanism, and integration into functionally distinct intracellular scaffolds. *Annu. Rev. Biochem.* 73:749–789.

Herrmann, H., M. Haner, M. Brettel, S.A. Muller, K.N. Goldie, B. Fedtke, A. Lustig, W.W. Franke, and U. Aebi. 1996. Structure and assembly properties of the intermediate filament protein vimentin: the role of its head, rod and tail domains. *J. Mol. Biol.* 264:933–953.

Herrmann, H., M. Haner, M. Brettel, N.O. Ku, and U. Aebi. 1999. Characterization of distinct early assembly units of different intermediate filament proteins. *J. Mol. Biol.* 286:1403–1420.

Herrmann, H., H. Bar, L. Kreplak, S.V. Strelkov, and U. Aebi. 2007. Intermediate filaments: from cell architecture to nanomechanics. *Nat. Rev. Mol. Cell Biol.* 8:562–573.

Holwell, T.A., S.C. Schweitzer, and R.M. Evans. 1997. Tetracycline regulated expression of vimentin in fibroblasts derived from vimentin null mice. *J. Cell Sci.* 110:1947–1956.

Kim, S., and P.A. Coulombe. 2007. Intermediate filament scaffolds fulfill mechanical, organizational, and signaling functions in the cytoplasm. *Genes Dev.* 21:1581–1597.

Kirmse, R., S. Portet, N. Mucke, U. Aebi, H. Herrmann, and J. Langowski. 2007. A quantitative kinetic model for the in vitro assembly of intermediate filaments from tetrameric vimentin. *J. Biol. Chem.* 282:18563–18572.

Lee, M.K., Z. Xu, P.C. Wong, and D.W. Cleveland. 1993. Neurofilaments are obligate heteropolymers in vivo. *J. Cell Biol.* 122:1337–1350.

Lodish, H., A. Berk, C. Kaiser, M. Krieger, M.P. Scott, A. Bretscher, H. Ploegh, and P. Matsudaira. 2008. Molecular Cell Biology. Sixth edition. W.H. Freeman and Company, New York. 1150 pp.

Mucke, N., T. Wedig, A. Burer, L.N. Marekov, P.M. Steinert, J. Langowski, U. Aebi, and H. Herrmann. 2004. Molecular and biophysical characterization of assembly-starter units of human vimentin. *J. Mol. Biol.* 340:97–114.

Murphy, D.B., R.O. Gray, W.A. Grasser, and T.D. Pollard. 1988. Direct demonstration of actin filament annealing in vitro. *J. Cell Biol.* 106:1947–1954.

Ngai, J., T.R. Coleman, and E. Lazarides. 1990. Localization of newly synthesized vimentin subunits reveals a novel mechanism of intermediate filament assembly. *Cell*. 60:415–427.

Parry, D.A., S.V. Strelkov, P. Burkhard, U. Aebi, and H. Herrmann. 2007. Towards a molecular description of intermediate filament structure and assembly. *Exp. Cell Res.* 313:2204–2216.

Patterson, G.H., and J. Lippincott-Schwartz. 2002. A photoactivatable GFP for selective photolabeling of proteins and cells. *Science*. 297:1873–1877.

Prahlad, V., M. Yoon, R.D. Moir, R.D. Vale, and R.D. Goldman. 1998. Rapid movements of vimentin on microtubule tracks: kinesin-dependent assembly of intermediate filament networks. *J. Cell Biol.* 143:159–170.

Rothwell, S.W., W.A. Grasser, and D.B. Murphy. 1986. End-to-end annealing of microtubules in vitro. *J. Cell Biol.* 102:619–627.

Sarria, A.J., S.K. Nordeen, and R.M. Evans. 1990. Regulated expression of vimentin cDNA in cells in the presence and absence of a preexisting vimentin filament network. *J. Cell Biol.* 111:553–565.

Shaner, N.C., R.E. Campbell, P.A. Steinbach, B.N. Giepmans, A.E. Palmer, and R.Y. Tsien. 2004. Improved monomeric red, orange and yellow fluorescent proteins derived from *Discosoma* sp. red fluorescent protein. *Nat. Biotechnol.* 22:1567–1572.

Soellner, P., R.A. Quinlan, and W.W. Franke. 1985. Identification of a distinct soluble subunit of an intermediate filament protein: tetrameric vimentin from living cells. *Proc. Natl. Acad. Sci. USA*. 82:7929–7933.

Sokolova, A.V., L. Kreplak, T. Wedig, N. Mucke, D.I. Svergun, H. Herrmann, U. Aebi, and S.V. Strelkov. 2006. Monitoring intermediate filament assembly by small-angle x-ray scattering reveals the molecular architecture of assembly intermediates. *Proc. Natl. Acad. Sci. USA*. 103:16206–16211.

Vikstrom, K.L., S.-S. Lim, R.D. Goldman, and G.G. Borisy. 1992. Steady state dynamics of intermediate filament networks. *J. Cell Biol.* 118:121–129.

Wickert, U., N. Mucke, T. Wedig, S.A. Muller, U. Aebi, and H. Herrmann. 2005. Characterization of the in vitro co-assembly process of the intermediate filament proteins vimentin and desmin: mixed polymers at all stages of assembly. *Eur. J. Cell Biol.* 84:379–391.

Woll, S., R. Windoffer, and R.E. Leube. 2005. Dissection of keratin dynamics: different contributions of the actin and microtubule systems. *Eur. J. Cell Biol.* 84:311–328.

Yamamichi-Nishina, M., T. Ito, T. Mizutani, N. Yamamichi, H. Watanabe, and H. Iba. 2003. SW13 cells can transition between two distinct subtypes by switching expression of BRG1 and Brm genes at the post-transcriptional level. *J. Biol. Chem.* 278:7422–7430.